

## Tunable Photophysical Properties of Two 2,2'-Bipyridine-Substituted Pyrene Derivatives

Tirapattur Soujanya, Annie Philippon, Stéphanie Leroy, Martine Vallier, and Frédéric Fages\*

Group of Supramolecular Chemistry and Catalysis, Laboratoire de Chimie Organique et Organométallique, LCOO UMR 5802 CNRS, Université Bordeaux I, 33405 Talence Cedex, France

Received: February 18, 2000; In Final Form: June 28, 2000

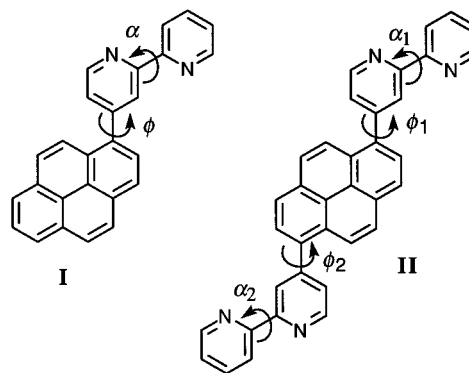
Two fluorescent pyrene derivatives, **I** and **II**, are reported in which the aromatic ring is connected to the 2,2'-bipyridine (bpy) complexing unit via a single C–C bond. Compound **I** contains one bpy moiety at the 1 position of the pyrene nucleus while **II** bears two bpy moieties linked to the 1 and 6 vertexes. The solvent-polarity dependence of the fluorescence emission properties of both compounds at room temperature points to the existence of a polar excited-state possessing a small extent of intramolecular charge transfer (ICT). The large fluorescence quantum yields,  $\Phi_f$ , the high radiative rate constants,  $k_f$ , and the short fluorescence lifetimes,  $\tau_f$ , for both compounds are characteristic of strongly allowed transitions. The solvent and temperature dependence of the photophysical properties of **I**, such as the increase of  $k_f$  with increasing polarity and temperature, appears to be due to intermixing between closely lying polar  $S_1(^1L_a)$  and forbidden  $S_2(^1L_b)$  states. Semiempirical theoretical calculations were performed for **I** and allowed to confirm the assignment of the electronic and structural nature of the two lowest-energy excited states as a function of the interannular dihedral angle. In contrast, the experimental and calculated properties for compound **II** point to the occurrence of a highly stabilized  $^1L_a$ -type excited state, thus experiencing very little influence of the forbidden  $^1L_b$ -type state. Consistently, the fluorescence emission rate constant for **II** is found to be independent of solvent polarity and temperature

### 1. Introduction

The design and synthesis of highly fluorescent compounds with tunable emission properties is one of the major challenges for the development of chemosensors and molecular-scale photonic devices.<sup>1,2</sup> A common feature of the majority of systems reported to date is that their structure is based on the covalent linking of a fluorophore moiety to a chelating unit, which allows one to monitor the interplay between fluorescence emission and metal cation complexation.<sup>3</sup> In that connection, we reported a series of molecular receptors for transition metal ions in which the pyrene chromophore is connected to a complexation site via a flexible, nonconjugated tether.<sup>4–6</sup> These systems were shown to display fluorescence emission properties highly sensitive to the presence of metal cation and, thus, to act as efficient reporter molecules for metal species in solution. Particularly those pyrene-containing ligands based on 2,2'-bipyridine (bpy) proved to be particularly interesting for they further enabled to build up ruthenium(II) tris(diimine) species, thereby leading to the generation of bichromophoric pyrene–Ru(bpy)<sub>3</sub><sup>2+</sup> dyads with outstanding photophysical properties. Indeed, recent publications have shown that among the number of Ru(bpy)<sub>3</sub><sup>2+</sup>-incorporating dyads bearing a pendant polycyclic aromatic moiety, those based on the pyrene chromophore were of particular interest due to the quasi isoenergetic position of the triplet excited states of the metal complex and the pyrene moiety.<sup>7–11</sup> This peculiar feature allows for reversible triplet–triplet energy transfer to take place efficiently between the two partners, the result of which being an extraordinary extension of the <sup>3</sup>MLCT lifetime of the Ru(bpy)<sub>3</sub><sup>2+</sup> chromophore.

Recently, we reported the synthesis and the preliminary photophysical study of the pyrene-bpy ligand, **I**, in which the

CHART 1



aromatic hydrocarbon and heterocyclic moieties are connected via a single C–C bond (Chart 1).<sup>12</sup> Direct substitution was anticipated to ensure significant electronic communication between subunits and also to increase the stabilization of the allowed  $^1L_a$  state of pyrene in order to provide high fluorescence efficiency as compared to the related alkyl chain-bridged two-component systems in which the lowest electronic energy state is of  $^1L_b$  type. During the course of our investigation, Schmehl and co-workers reported the spectroscopic properties of the ruthenium(II) tris(diimine) complex of **I**, and they found a very long-lived <sup>3</sup>MLCT luminescence (ca. 50  $\mu$ s) at room temperature in acetonitrile.<sup>8</sup> In the same connection, Harriman and Zissel reported the case of a photoactive dyad in which the pyrene and bpy fragments are bridged by an ethynylene spacer.<sup>11,13</sup>

These recent studies illustrate the interest of such conjugated pyrene-bpy structures as light-sensitive ligand units on which to base the design of photoactive supramolecular metallosystems. This motivated us to synthesize the ditopic ligand **II**, in which two bpy units are connected via a single C–C bond to

\* To whom correspondence should be addressed. E-mail: f.fages@lcoo.u-bordeaux.fr.

the 1 and 6 positions of the pyrene nucleus (Chart 1). This triad compound was anticipated to enable the synthesis of homo- and heterobinuclear metal complexes and thus to offer a unique opportunity to study reversible, triplet–triplet electronic energy transfer between the three chromophores all over the oligomeric structure.<sup>14,15</sup>

Moreover, conjugated pyrene-bpy ligands belong to that class of fluorescent dipolar biaryl molecules that combine intramolecular charge transfer (ICT) emission and metal complexation. Typically, dipolar molecules in which strong donor and acceptor groups are conjugated via a  $\pi$  system are known to display a large dipole moment difference in the ground and excited states.<sup>16</sup> Following excitation, the locally excited state in many of such systems undergoes relaxation to a highly polar emitting state, which leads to either a dual fluorescence emission or a single fluorescence emission with large Stokes shifts.<sup>17–24</sup> ICT fluorophores appeared as photosensitive units of choice to be incorporated into supramolecular structures endowed with molecular recognition properties.<sup>2</sup> As an example, a family of D– $\pi$ –A stilbenes substituted with a *N*-monoaza-crown-ether macrocycle as donor unit were shown to act as sensitive probes toward light metal cations and, particularly, Ca<sup>2+</sup> metal ion.<sup>25,26</sup> D/A molecules bearing the pyrene chromophore and either a strong donor (dimethylamino)<sup>22,27</sup> or acceptor (acetophenone)<sup>28</sup> were reported to exhibit a single fluorescence band with large Stokes shifts rather than a dual emission. In the case of compound **I**, the preliminary results<sup>12</sup> pointed to the contribution of a rather weakly polar excited state to account for the comparatively small Stokes shift, consistently with the weak electron-withdrawing effect of the bpy substituent.

The main purpose of this study is to provide better insights into the knowledge of the photophysical properties of pyrene-bpy dyads in relation to the excited-state behavior of their corresponding metalated systems. Particularly, it is desirable to get a clear picture of the electronic nature and conformational properties of the lowest-energy singlet excited state of the free ligands **I** and **II** following excitation into the pyrene moiety. Moreover, besides its potential interest as molecular wire for bridging two metal centers, free ligand **II** also represents a new  $\pi$ -extended system in which the pyrene chromophore is symmetrically substituted with two acceptor bpy units. The properties of pyrene derivatives substituted with one aromatic nucleus have been investigated recently.<sup>29</sup> Highly symmetrical molecules displaying large quadrupolar or octupolar contribution are of main interest in many areas.<sup>30</sup>

In this paper we report the steady-state and time-resolved fluorescence emission properties of the free ligands **I**, as they were not reported previously,<sup>8,12</sup> and **II**. Particularly the effects of solvent polarity and temperature were investigated. It is well-known that the angle of torsion around the C–C bond between donor and acceptor moieties is a structural parameter that has a profound effect on ground- and excited-state properties of dipolar molecules.<sup>17–28</sup> Therefore the influence of the interannular dihedral angle,  $\phi$ , between pyrene and bpy units (Chart 1) on the calculated properties of the two lowest-energy excited states in **I** and **II** was investigated using semiempirical calculations in order to support the experimental data.

## 2. Experimental Section

**2.1. Syntheses.** The synthesis of compound **I** has been described elsewhere.<sup>12</sup> The bis(bipyridinyl)pyrene derivative, **II**, was synthesized via a palladium-catalyzed cross-coupling reaction between pyrene-1,6-diylboronic<sup>31a</sup> acid and 4-bromo-2,2'-bipyridine<sup>31b</sup> in DMF (100 °C, 12 h) using 10 mol % of

dichlorobis(triphenylphosphine)palladium(II) as catalyst and CaCO<sub>3</sub> as a base. Compound **II** was purified by successive crystallizations in chloroform and obtained in 60% yield as pale beige solid. Compound **II** gave satisfactory <sup>1</sup>H NMR spectroscopy and mass spectrometry data. Anal. Calcd for C<sub>36</sub>H<sub>22</sub>N<sub>4</sub>·2H<sub>2</sub>O: C, 79.68; H, 4.83; N, 10.32. Found: C, 79.65; H, 4.71; N, 9.21.

**2.2. Spectroscopic Studies.** All solvents for spectroscopic measurements were purified by standard procedures. Following are the abbreviations used for the solvents: *n*-hexane (HEX); toluene (TOL); tetrahydrofuran (THF); 2-methyltetrahydrofuran (MTHF); propionitrile (PN); butyronitrile (BN); acetonitrile (AN); *n*-propanol (PrOH); ethanol (EtOH); methanol (MeOH). UV–vis spectra were recorded on a Hitachi U3300 spectrophotometer, and fluorescence spectra, either on a Hitachi F4500 or a Spex Fluorolog spectrofluorometer. Fluorescence decays were obtained using a single photon timing apparatus as described elsewhere.<sup>32</sup> Low-temperature experiments were carried out using a variable-temperature liquid nitrogen Optistat cryostat from Oxford instruments. We did not find any difference in emission properties with and without degassing the solutions. Fluorescence quantum yields were determined using quinine sulfate as a standard ( $\Phi_f = 0.55$  at 25 °C in 1 N H<sub>2</sub>SO<sub>4</sub>).<sup>33,34</sup> The relative error of the quantum yields is  $\pm 5\%$ . Ligand concentration dependence on the emission properties was examined and allowed to show the absence of chromophore aggregation for **I** and **II** at concentrations below 10<sup>−6</sup> M.

**2.3. Quantum Chemical Calculations.** The input geometries were first fully optimized at different twist angles of bipyridine unit with respect to pyrene at intervals of 10°, using the AM1 Hamiltonian within the AMPAC program.<sup>35</sup> The excited-state energies were obtained for each optimized ground-state geometry using full configuration interaction in which 585 microstates were kept using the Moller–Plesset presort scheme.<sup>35</sup> The potential energies of the first two excited states, S<sub>1</sub>(<sup>1</sup>L<sub>a</sub>) and S<sub>2</sub>(<sup>1</sup>L<sub>b</sub>), were obtained by combining the ground-state potential obtained from AM1 calculations with the gas-phase excitation energies according to<sup>17</sup>

$$E(S_n) = E_{\text{gas}}(S_0) + \Delta E(S_0 \rightarrow S_n) \quad (1)$$

Due to the large uncertainty in defining the Onsager cavity radius of elongated molecules, the solvent stabilization energy was not taken into account in eq 1. For the same reason, we did not attempt to calculate the dipole moment value from the solvatochromic shift.

## 3. Results and Discussion

**3.1. Electronic Absorption and Steady-State Fluorescence Emission.** The absorption and steady-state fluorescence spectra are shown in Figures 1 and 2, respectively, for **I** and **II** in solvents of different polarity. As can be seen from Figure 1, the longest-wavelength absorption band for both compounds is broad relative to that of 1-alkylpyrene derivatives which are known to exhibit well-separated vibronic bands.<sup>27,36</sup> It is also found to be red-shifted as a result of a strong electronic interaction between pyrene and bipyridine through  $\pi$  conjugation. This effect is particularly pronounced for ligand **II**, the lowest-energy transition band being found to be more red-shifted (+20 nm) and broader than that in **I**, probably due to an extended conjugation pathway all over the triad molecule **II** in the ground state. The absorption and fluorescence emission data as a function of the solvent polarity are collected in Table 1.

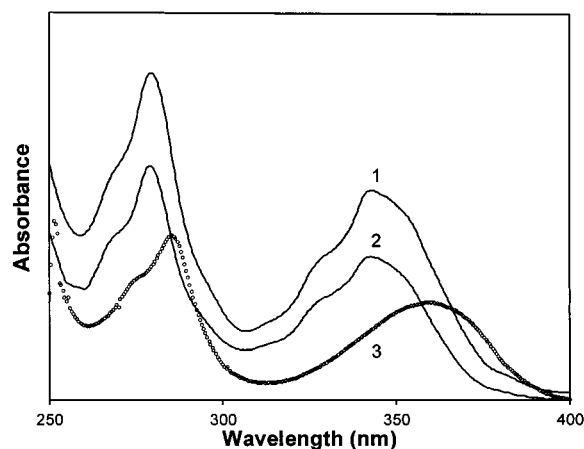


**Figure 1.** Electronic absorption spectra of **I** in *n*-hexane (1) and acetonitrile (2) and **II** in acetonitrile (3) at room temperature.

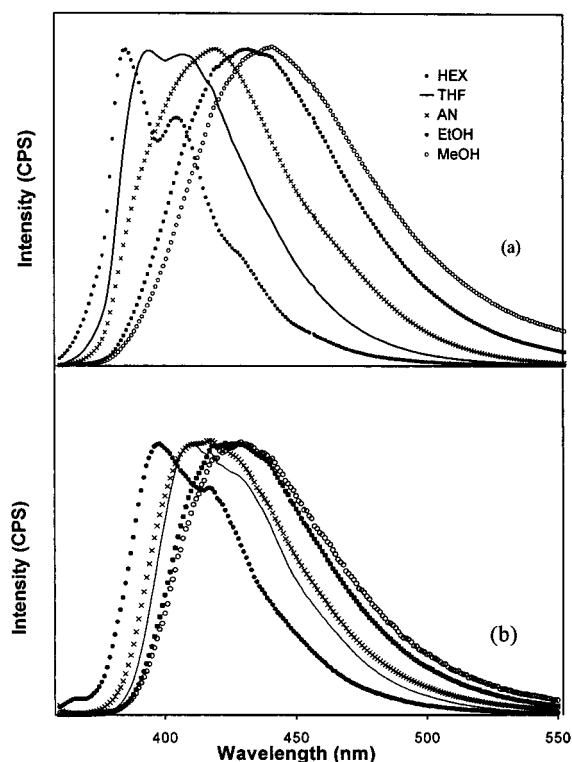


**Figure 2.** Normalized fluorescence emission spectra of (a) **I** and (b) **II** in solvents of different polarity at 298 K ( $\lambda_{\text{exc}} = 340$  nm for **I** and 360 nm for **II**,  $<5 \times 10^{-7}$  M).

They indicate that the position of the absorption maximum for **I** and **II** does not change with the polarity, not even in the protic solvents. The molar absorption coefficient of the lowest-energy transition band is found to be around  $25\,000\text{ M}^{-1}\text{ cm}^{-1}$  for **I** (at 342 nm) and  $40\,000\text{ M}^{-1}\text{ cm}^{-1}$  for **II** (at 361 nm) in all the solvents investigated. This is much higher than for pyrene and its 1-substituted derivatives that are known to possess a forbidden  $^1\text{L}_b$  state as lowest-energy excited state. Therefore the lowest-energy transition in **II** is not due to the pure forbidden  $^1\text{L}_b$  and is likely to emanate from a  $^1\text{L}_a$ -type state. The situation appears to be somewhat more complex in the case of ligand **I** as a shoulder at 380 nm is detected in the low-polarity solvent hexane but not in the polar solvents (Figure 1). This suggests the occurrence of a low-lying  $^1\text{L}_b$  state in nonpolar medium.

For all the solvents, the corrected fluorescence emission spectra of **I** and **II** are found to be independent of the excitation wavelength. In contrast to electronic absorption, the fluorescence

**TABLE 1: Spectroscopic Data for I and II in Solvents of Different Polarity at 298 K: Absorption and Fluorescence Transition Energy Maxima  $\nu_a$  and  $\nu_f$  and Stokes Shifts  $\Delta\nu_{\text{st}}$  (All in  $\text{cm}^{-1}$ )**

solvent <sup>a</sup>	$\epsilon^b$	$\nu_a$	$\nu_f$	$\Delta\nu_{\text{st}}$
Compound <b>I</b>				
HEX	1.92	29240	25974	3266
TOL	2.27	29155	25445	3709
THF	7.58	29070	25381	3689
BN	20.3	29070	24510	4560
PN	28.86	29155	24510	4645
AN	35.94	29155	24390	4764
PrOH	20.45	29155	23310	5844
EtOH	24.6	29155	23202	5953
MeOH	32.66	29155	22831	6323
Compound <b>II</b>				
HEX	1.92	27701	25126	2575
TOL	2.27	27624	24380	3244
THF	7.58	27624	24510	3114
BN	20.3	27778	24510	3268
PN	28.86	27778	24510	3268
AN	35.94	27778	23923	3855
PrOH	20.45	27701	23310	4391
EtOH	24.6	27701	23256	4445
MeOH	32.66	27548	23256	4292

<sup>a</sup> The solvent abbreviations are given in the Experimental Section.  
<sup>b</sup>  $\epsilon$  is the static dielectric constant of the solvent taken from ref 47.

spectra in nonpolar solvents display a vibrational structure and a narrow half-height width, a value of  $2417\text{ cm}^{-1}$  ( $3030\text{ cm}^{-1}$ ) being found for **I** (**II**) instead of  $3372\text{ cm}^{-1}$  ( $3890\text{ cm}^{-1}$ ) for the corresponding absorption band in HEX. This points to a narrower distribution of rotamers in the excited state with different interannular twist angles between pyrene and bpy fragments. An increase in solvent polarity is observed to lead to a red shift and an increase of the half-height width ( $4651\text{ cm}^{-1}$  for **I** and  $3630\text{ cm}^{-1}$  for **II** in AN) of the emission band (Figure 2). The solvatochromic effect is characteristic of the emission from a polar excited state with a dipole moment that is bigger than that of the ground state. The Stokes shift values in all the solvents and the Stokes shift difference between HEX and AN are found to be smaller for **II** than for **I**. This indicates that the solvent-equilibrated excited state is less polar in **II** than in **I**, consistently with the symmetric structure of the former. The magnitude of Stokes shift difference observed from hexane to acetonitrile in the more polar compound **I** ( $1498\text{ cm}^{-1}$ ) is considerably less than for related donor/acceptor systems incorporating the pyrene chromophore.<sup>22,27,28</sup> Particularly it is worth noting that the extent of charge transfer is also found to be less than in the related dyad in which pyrene and bpy moieties are bridged by a triple bond.<sup>13</sup> Indeed the emission band for the latter system was shown to be subject to a considerable Stokes shift. This was attributed to the presence of the ethynylene spacer acting as an electron-withdrawing substituent, which contributed to increase the stabilization of the ICT state relative to the locally excited one. Fluorescence emission in **I**, and a fortiori in **II**, is thus anticipated to occur to a larger extent from a locally excited-state having a high  $\pi\pi^*$  character and less ICT contribution relative to the ethynylene-bridged compound.<sup>13</sup> This is further substantiated by evaluating the exothermicity of the charge separation process in **I**,  $\Delta G_0$ , using the Rehm–Weller equation.<sup>37</sup> The calculated value, using electrochemical data found in the literature,<sup>38</sup> is found to be slightly negative, indicating that there is really not a large driving force in polar solvents for charge transfer to take place from the excited pyrene donor to the bipyridine acceptor.

Specific interactions with alcohol solvent molecules are known to increase ICT. Unlike the absorption spectra, the



TABLE 2: Photophysical Properties of I and II at 298 K<sup>a</sup>

solvent	$\Phi_f$	$\tau_f$	$k_{nr}$	$k_f$	$k_f/\nu_f^3 n^3$	$f \epsilon d\nu_a$	$k_f/k_f^{SB}$
Compound I							
HEX	0.48	8.1	6.4	6.0	12.8	1.0	0.2
TOL	0.52	6.0	8.0	8.8	15.8		
THF	0.47	6.5	8.1	7.2	15.8	0.9	0.4
BN	0.56	5.5	8.1	10.1	27.0		
PN	0.62	4.6	8.2	13.6	36.2		
AN	0.64	4.7	7.6	13.7	38.9	1.0	0.5
PrOH	0.56	3.5	12.7	16.2	48.1		
EtOH	0.66	3.5	9.8	18.8	59.7		
MeOH	0.15	3.1	27.4	4.7	16.8		
Compound II							
HEX	0.60	2.6	15.3	23.0	80.0		
TOL	0.56	1.8	24.4	31.3	80.7		
THF	0.65	2.0	17.4	32.7	65.6		1.5
BN	0.58	2.1	20.2	27.2	69.6		
PN	0.56	2.2	20.4	26.0	69.8		
AN	0.56	2.2	20.0	25.0	75.2		
PrOH	0.38	2.1	29.4	17.8	52.8		
EtOH	0.39	2.1	28.9	18.3	57.7		
MeOH	0.27	1.7	44.0	16.6	52.3		

<sup>a</sup> Fluorescence quantum yields  $\Phi_f$ , fluorescence lifetimes  $\tau_f$  (ns), nonradiative  $k_{nr} = (1 - \Phi_f)/\tau_f$  ( $10^7$  s<sup>-1</sup>) and radiative rate constants  $k_f$  ( $10^7$  s<sup>-1</sup>), reduced radiative rates  $k_f/\nu_f^3 n^3$  ( $10^{-7}$  s<sup>-1</sup> cm<sup>3</sup>), integrated areas of lowest-energy absorption band  $f \epsilon d\nu_a$  (M<sup>-1</sup> cm<sup>-2</sup>), ratios of fluorescent rate to Strickler–Berg rate constants  $k_f/k_f^{SB}$  (see text). No table entry means not determined.

fluorescence emission bands of both derivatives are very sensitive to the protic character of the solvent. The effect of hydrogen bonding to the bpy nitrogen atoms is to produce an additional red-shift and a broadening of the emission band (Figure 2, Table 1), as evidenced by comparing the data for solvents of same polarity but of different proticity, such as butyronitrile ( $\epsilon = 20.3$ ) and *n*-propanol ( $\epsilon = 20.4$ ).

**3.2. Room-Temperature Photophysics.** The photophysical data for **I** and **II** are collected in Table 2. The fluorescence quantum yields for **II** are found to be in the range of 0.55–0.60, independent of the polarity, and smaller in protic solvents relative to the corresponding equipolar but aprotic solvent. The fluorescence lifetimes for **II** are monoexponential in the nanosecond regime, a constant value of 2 ns being measured in all the solvents. To exclude the effect of the wavelength dependence on the emission probability, reduced rate constants,  $k_f/n^3\nu_f^3$ , were calculated according to eq 2:<sup>18,41</sup>

$$k_f = \frac{64\pi^4}{3h} n^3 \nu_f^3 M_f^2 \quad (2)$$

The reduced  $k_f$  values for **II** are thus found to be higher than those for **I** and to remain constant with solvent polarity. These observations support that fluorescence emission in **II** is a strongly allowed process originating from a  $\pi\pi^*$  singlet excited state having a strong <sup>1</sup>L<sub>a</sub> character irrespective of the solvent polarity. Indeed the substitution on both the 1 and 6 positions of the pyrene is known to induce a stabilization of the long-axis polarized transition.<sup>42</sup> Further information can be derived from the consideration of the ratio given in eq 5, which is independent of  $\nu_f$  and  $n$ , and obtained by substituting eq 4 in eq 3:<sup>18,43</sup>

$$k_f^{SB} = \frac{8\pi c 10^3 \ln 10}{N_L} n^2 \nu_f^3 \int \epsilon(\nu_a) d(\ln \nu_a) \quad (3)$$

where

$$\int \epsilon(\nu_a) d(\ln \nu_a) = \frac{8\pi^3 N_L n}{3hc 10^3 \ln 10} M_a^2 \quad (4)$$

Therefore,

$$\frac{k_f}{k_f^{SB}} = \frac{M_f^2}{M_a^2} \quad (5)$$

This ratio allows the comparison between the fluorescence rate constant,  $k_f$ , determined experimentally, and the one obtained from the electronic absorption spectrum using the Strickler–Berg equation (eq 3).<sup>41</sup> A ratio value deviating from unity is found for **II** in THF, indicating a change of electronic or conformational structure taking place in the excited-state S<sub>1</sub>. According to the fluorescence data (vide supra), this effect is to be related to excited-state angular relaxation. The value of 1.5 for the ratio in eq 5 points to the presence of a distribution of rotamers in S<sub>1</sub> with more planar geometries and having a transition dipole moment ( $M_f$ ) higher than in S<sub>0</sub> ( $M_a$ ).

The photophysical study of the mono(bipyridyl) ligand, **I**, allowed us to point to a significantly different behavior. The higher Stokes shift values for **I** relative to **II** (Table 1) indicate that angular relaxation processes are more effective in the excited state of the former relative to the latter. The fluorescence quantum yields obtained for **I** are also found to be significantly high (50–60%) but to increase with solvent polarity (Table 2). The fluorescence decay curves in all the solvents are monoexponential on the nanosecond time scale and found to be same at all the wavelengths monitored. Noteworthy is the significant and constant increase of the experimental and reduced  $k_f$  values of **I** with increasing polarity of the aprotic solvents, the value of the reduced radiative rate constant in acetonitrile being about 3 times higher than in hexane. Conversely, the nonradiative rate,  $k_{nr}$ , shows no polarity dependence. According to eq 2, an increase of the reduced radiative rate directly reflects an increase in the fluorescence transition moment  $M_f$  as a function of solvent polarity. The ratio value obtained from eq 5 reaches less than unity (Table 2) and increases with solvent polarity as a consequence of the higher emission probability in more polar solvents as outlined above. These results point to a change in electronic and/or molecular structure occurring between the absorption and the emission process, the fluorescence transition being less allowed than the absorption process. Moreover the integrated absorption intensity,  $f \epsilon d\nu_a$ , which is proportional to the oscillator strength,  $f$ , is found to be same in all the solvents measured (Table 2). This indicates that the electronic and structural properties of the ground and Franck–Condon excited state responsible for the first absorption band in **I** do not change with the polarity. Given this, it is inferred that it is the nature of the emitting excited state that is solvent sensitive. Two possibilities can account for this effect: (i) a quantum chemical mixing of closely lying allowed <sup>1</sup>L<sub>a</sub>-type and forbidden <sup>1</sup>L<sub>b</sub>-type excited states, leading to a mixed wave function for a single conformation; (ii) a rotamer distribution in the excited state, which is polarity dependent and different from that prevailing in the ground state.

Finally, the  $k_{nr}$  values for both compounds are found to be larger in protic solvents than in nonprotic ones (Table 2), which is consistent with the existence of additional radiationless deactivation channels as generally observed in the case of specific solvent–solute interactions involving ICT molecules. Protonation or coordination of zinc(II) at the nitrogen sites of

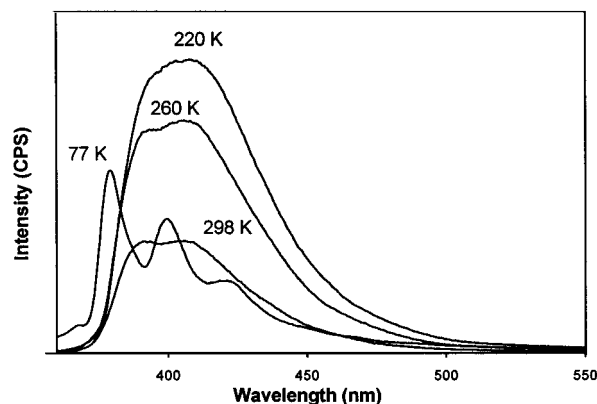


**Figure 3.** Fluorescence emission spectra of **I** in MTHF at different temperatures.

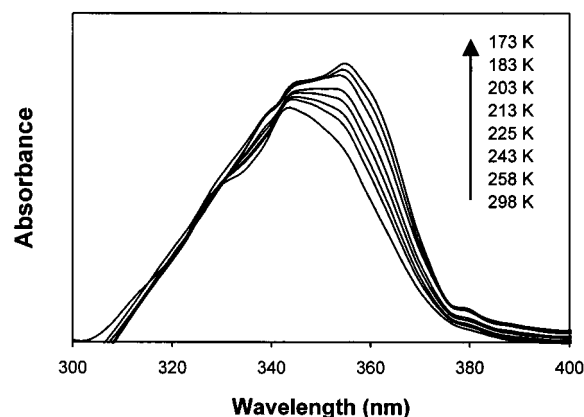


**Figure 4.** Absorption spectra of **I** in MTHF as a function of temperature.

the bpy unit was shown to induce the quantitative quenching of fluorescence for both **I** and **II** in acetonitrile. This is due to facile ICT formation resulting from the enhanced electron-withdrawing effect of the proton- or metal-bound bpy ligand.

**3.3. Low-Temperature Electronic Absorption and Fluorescence Emission.** The absorption and fluorescence emission measurements at low temperature were done in the medium polar solvent, 2-methyltetrahydrofuran (MTHF). The fluorescence spectra of **I** and **II** in MTHF (Figure 3) exhibit an increase in intensity and a slight bathochromic shift with decreasing temperature with respect to those recorded at room temperature, the latter effect being probably due to the slight increase in polarity with decreasing temperature. At all the temperatures above the melting point of the solvent, the emission spectra are found to be same irrespective of excitation wavelength. Decreasing the temperature caused a red-shift and structuring of the fluorescence excitation spectrum. In the case of **I**, the fluorescence excitation spectra match the corresponding absorption spectra. Indeed, a hyperchromic effect and a bathochromic shift for the longest-wavelength absorption band, along with its structuring, can be observed as the temperature is gradually decreased (Figure 4). This is due to the existence of a temperature-dependent conformational distribution in the ground state.<sup>27</sup> In rigid solvent glass at low temperature (77 K), the fluorescence emission spectra of both compounds are shifted to higher energy and show the well-structured vibronic bands in agreement with the lack of solvent relaxation in rigid medium.

The lifetime value of ligand **II** was found to be independent of the temperature, a constant value of the radiative rate constant  $k_f$  being obtained. The situation is quite different in the case of **I**. The fluorescence quantum yields at various temperatures,

**TABLE 3: Temperature Dependence of the Photophysical Data of **I** in MTHF<sup>a</sup>**

temp, K	$\Phi_f$	$\tau_f$	$k_f$	$k_{nr}$	temp, K	$\Phi_f$	$\tau_f$	$k_f$	$k_{nr}$
300	0.52	6.5	8.0	7.3	230	0.87	5.6	15.5	2.4
290	0.58	6.0	9.6	7.1	220	0.88	5.5	16.0	2.2
280	0.62	6.0	10.4	6.3	210	0.91	5.0	18.3	1.7
270	0.68	6.1	11.0	5.3	200	0.91	4.8	18.9	1.9
260	0.72	5.8	12.4	4.8	190	0.93	4.7	20.0	1.5
250	0.77	5.9	13.0	3.9	180	0.94	4.0	20.8	1.5
240	0.80	5.7	14.1	3.4					

<sup>a</sup> See footnote *a* for Table 2.

corrected for the increase in absorbance (Table 3), are found to increase drastically with reducing temperature, reaching a value of almost unity at 180 K. Nanosecond time-scale single photon counting measurements were performed for **I** in the liquid phase of the solvent MTHF, from 300 to 180 K, and the decays were found to be perfectly monoexponential. The lifetime values are found to decrease significantly upon lowering the temperature, from 6.5 ns at room temperature to 4 ns at 180 K. Upon further cooling of the samples below the freezing temperature of the solvent, the fluorescence decays became multiexponential, indicating the emission from frozen conformers which cannot interconvert in rigid media. These data lead to the following unusual behavior that is an increase of the radiative rate when the temperature decreases. The temperature independence of the radiative rate in the molecular electronic transitions is generally taken as a rule.<sup>41</sup> One known exception however is the case of intramolecular full CT states in which fluorescence emission is thermally activated.<sup>44</sup> Actually we observed the opposite effect in the case of compound **I**.

The whole experimental data can be rationalized according to a two-state model, as demonstrated in previous studies on D/A systems in which intermixing between low-lying excited states was connected to the existence in solution of a distribution of rotamers.<sup>21,45</sup> Indeed, the lowest-energy state in compound **I** could mix into  $^1L_a$  and  $^1L_b$  components, the extent of intermixing being dependent on temperature and solvent polarity. Therefore, an increase of the  $^1L_a$  parentage at low temperature or in polar solvent could explain the enhancement of fluorescence emission probability in **I**, as expressed by  $k_f$ . In the case of compound **II**, the result of substitution at the 1 and 6 positions of the pyrene chromophore is to provide strong stabilization of the low-lying  $^1L_a$  state relative to the  $^1L_b$  state, thereby leading to the absence in **II** of intermixing. Consequently, the radiative rate is larger than for **I** and not sensitive to solvent polarity and temperature.

**3.4. Quantum Chemical Calculations.** Quantum chemical calculations were performed in order to validate the above-mentioned model and also to get some insights into the ground- and excited-state properties of compounds **I** and **II** as a function of the dihedral angle,  $\phi$ . From the MM3 optimized structure, the more stable conformation in **I** and **II** is found to contain the nonsubstituted pyridine ring twisted with respect to the other one by  $\alpha = 40^\circ$ . This value was kept constant in all the calculations.<sup>46</sup> In the case of ligand **II**, the angular conformational processes have to be described by two dihedral angles,  $\phi_1$  and  $\phi_2$ , if one fixes  $\alpha_1$  and  $\alpha_2$  at the ground-state value. However, the full theoretical description of the system remains too complicated and calculations were performed assuming  $\phi_1 = \phi_2$  and  $\alpha_1 = \alpha_2 = 40^\circ$ . Under these oversimplifying conditions, it was found that the energy gap between  $^1L_b$  and  $^1L_a$  states in **II** (ca. 0.25 eV) tends to be twist-angle-independent and larger than for **I** (0.02–0.1 eV), which indicates that these two states remain energetically well-separated in agreement with the experimental results.

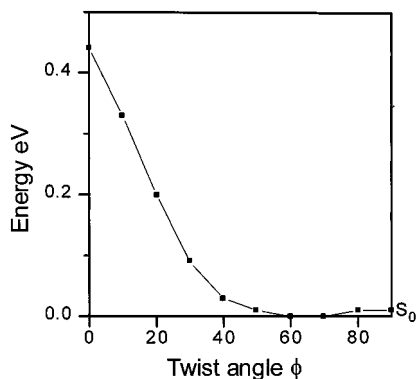


**Figure 5.** Dependence of the potential energy for **I** as a function of the twist angle between pyrene and bpy.

For compound **I**, the variation of the ground-state energy as a function of  $\phi$  is depicted in Figure 5, the value of  $\alpha$  being kept at  $40^\circ$ . It shows the existence of a rather flat minimum at ca.  $60^\circ$ , which is close to the twist angle value obtained for the lowest energy conformation of pyrene acetophenone.<sup>28</sup> A small barrier of about 10 meV appears at  $90^\circ$ . The rise in energy to reach the planar conformation in **I** is due to steric hindrances between peri and ortho hydrogen atoms in pyrene and bipyridine units. These observations confirm that a broad distribution of conformers prevails in the gas phase at room temperature between  $60$  and  $120^\circ$ . The broad angular distribution with small energy barriers in the ground state for **I** (Figure 5) allows one to confirm the temperature dependence of the electronic absorption spectrum of **I** (Figure 3). Indeed the red shift and structuring of the lowest-energy absorption band upon cooling is likely to originate from the narrowing of the Boltzmann distribution around more planar conformations.

The calculated potential energies, the dipole moments  $\mu$ , and the oscillator strengths  $f$  are plotted as function of the twist angle,  $\phi$ , for compound **I** in Figure 6a–c. The oscillator strengths (Figure 6c) and dipole moments (Figure 6b) of the  $S_1$  ( $^1L_a$ ) state are found to be higher than those of the  $S_2$  ( $^1L_b$ ) state in the gas phase. Moreover, the dipole moment values for  $S_1$  ( $^1L_a$ ) are relatively low (2–2.8 D) as compared to pyrene derivatives containing strong donor or acceptor groups.<sup>22,27,28</sup> This is consistent with the small experimental solvatochromic shift. Figure 6b shows that the more twisted is the geometry, the less polar is the  $S_1$  ( $^1L_a$ ) excited state. Due to the low values of energy barriers between sets of conformers (Figure 6a), the conformational distribution in  $S_1$  is expected to be broad and shifted toward more perpendicular geometries in the gas phase or in nonpolar solvents and, conversely, toward more planar species in dipolar solvents. It must be noted that the calculations suggest a flattening of the molecule in the excited state after relaxation from the Franck–Condon state, a situation which is thus more probable in more polar solvents. The interannular twist angle value is about  $40^\circ$ , instead of ca.  $60^\circ$  in the ground state, the energy barrier to reach the perpendicular geometry being around 90 meV. From Figure 6a, the energy gap between the allowed  $^1L_a$  and the forbidden  $^1L_b$  state is twist-angle-dependent and thus solvation-dependent. This supports a two-state model in which switching from a less allowed  $^1L_b$ -type to a more allowed  $^1L_a$ -type  $S_1$  emitting state is operative as the polarity is increased.

#### 4. Conclusion

This photophysical study allows one to characterize the properties of the weakly polar emitting excited state of two

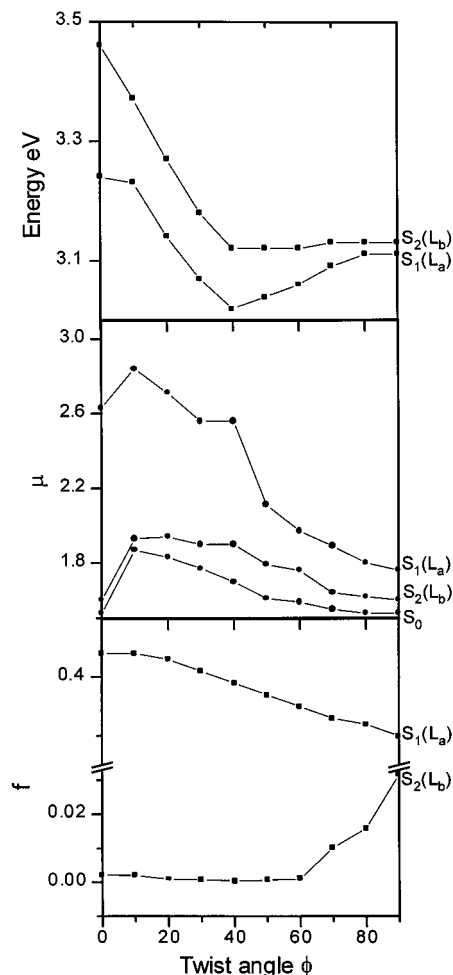


**Figure 6.** Twist angle-dependent calculated properties of the two low-lying excited states for **I** in the gas phase using fully optimized ground-state geometries: (a) potential energies according to eq 1; (b) excited-state dipole moment  $\mu$ , energies; (c) oscillator strength,  $f$ .

compounds, **I** and **II**, in which the pyrene nucleus is connected via a single C–C bond to one and two bipyridine units, respectively, as a weak electron acceptor group. Even in polar solvents, the ICT state is not strongly stabilized and the fluorescence emission in **I** and **II** is controlled by mixing between the allowed  $^1L_a$  and forbidden  $^1L_b$   $\pi\pi^*$  states of the aromatic chromophore. The extent of this interaction, and also the angular geometry of the excited state, are subject to the influence of temperature and solvent polarity, which allows one to fine-tune the fluorescence emission properties of **I**. Compound **II** presents a very high emission transition probability because the  $^1L_a$  state is greatly stabilized, experiencing thus little influence from the higher-energy  $^1L_b$  state. The bpy-substituted pyrene derivatives, especially the ditopic ligand **II**, appear as very promising engineered molecular systems endowed with fluorescence emission and complexation properties. They can serve as prototype structures for the development of new  $\pi$ -systems of well-defined shape and length with light-sensitive properties desirable for molecular photonic devices.

**Acknowledgment.** We thank Dr. L. Ducasse (University Bordeaux 1) for his help in theoretical calculations. We are grateful to Professor R. H. Schmehl and Dr A. Del Guizzo (Tulane University) for a critical reading of the manuscript and their insightful comments about the photophysical results. T.S. thanks the CNRS for granting a postdoctoral fellowship. The

CNRS, Université Bordeaux I, and La Région Aquitaine are gratefully acknowledged for financial support.

## References and Notes

- (1) *Chemosensors of Ion and Molecule Recognition*; Desvergne J.-P., Czarnik, A. W., Eds.; NATO ASI Series, Vol. 492; Kluwer Academic Publishers: Dordrecht, The Netherlands, 1997.
- (2) de Silva, A. P.; Gunaratne, H. Q. N.; Gunnlaugsson, T.; Huxley, A. J. M.; McCoy, C. P.; Rademacher, J. T.; Rice, T. E. *Chem. Rev.* **1997**, *97*, 1515.
- (3) de Silva, A. P.; Dixon, I. M.; Gunaratne, H. Q. N.; Gunnlaugsson, T.; Maxwell, P. R. S.; Rice, T. E. *J. Am. Chem. Soc.* **1999**, *121*, 1393.
- (4) Bodenant, B.; Weil, T.; Businelli-Pourcel, M.; Fages, F.; Barbe, B.; Planet, I.; Laguerre, M. *J. Org. Chem.* **1999**, *64*, 7034.
- (5) Bodenant, B.; Fages, F.; Delville, M.-H. *J. Am. Chem. Soc.* **1998**, *120*, 7511.
- (6) Sohna Sohna, J.-E.; Jaumier, P.; Fages, F. *J. Chem. Res., Synop.* **1999**, 134.
- (7) Sohna Sohna, J.-E. Ph.D. Thesis, University Bordeaux I, No. 1769, Bordeaux, France, 1997.
- (8) Simon, J. A.; Curry, S. L.; Schmehl, R. H.; Schatz, T. R.; Piotrowiak, P.; Jin, X.; Thummel, R. P. *J. Am. Chem. Soc.* **1997**, *119*, 11012.
- (9) (a) Ford, W. E.; Rodgers, M. A. J. *J. Phys. Chem.* **1992**, *96*, 2917. (b) Wilson, G. J.; Launikonis, A.; Sasse, W. H. F.; Mau, A. W.-H. *J. Phys. Chem. A* **1997**, *101*, 4860.
- (10) Baba, A. I.; Shaw, J. R.; Simon, J. A.; Thummel, R. P.; Schmehl, R. H. *Coord. Chem. Rev.* **1998**, *171*, 43.
- (11) Hissler, M.; Harriman, A.; Khatyr, A.; Ziessel, R. *Chem. Eur. J.* **1999**, *5*, 3366.
- (12) Rodriguez, A. L.; Peron, G.; Duprat, C.; Vallier, M.; Fouquet, E.; Fages, F. *Tetrahedron Lett.* **1998**, *39*, 1179.
- (13) Harriman, A.; Hissler, M.; Ziessel, R. *Phys. Chem. Chem. Phys.* **1999**, *1*, 4203.
- (14) (a) Harriman, A.; Ziessel, R. *J. Chem. Soc., Chem. Commun.* **1996**, 1707. (b) Schlicke, B.; Belser, P.; De Cola, L.; Sabbioni, E.; Balzani, V. *J. Am. Chem. Soc.* **1999**, *121*, 4207. (c) Sauvage, J.-P.; Collin, J.-P.; Chambron, J.-C.; Guillerez, S.; Coudret, C. *Chem. Rev.* **1994**, *94*, 993.
- (15) The copper(I)-induced self-assembly of a 1,8-bis(phenanthrolyl)-pyrene derivative has been reported: Bonnefous, C.; Bellec, N.; Thummel, R. P. *J. Chem. Soc., Chem. Commun.* **1999**, 1243.
- (16) (a) Rettig, W. *Angew. Chem., Int. Ed. Engl.* **1986**, *25*, 971. (b) Rettig, W. Electron-Transfer I. In *Topics in Current Chemistry*; Mattay, J., Ed.; VCH: New York, 1994; Vol. 169, p 253.
- (17) Cornelissen-Gude, C.; Rettig, W. *J. Phys. Chem. A* **1998**, *102*, 7754.
- (18) Maus, M.; Rettig, W.; Bonafoux, D.; Lapouyade, R. *J. Phys. Chem. A* **1999**, *103*, 3388.
- (19) Létard, J.-F.; Lapouyade, R.; Rettig, W. *J. Am. Chem. Soc.* **1993**, *115*, 2441.
- (20) Herbich, J.; Waluk, J. *Chem. Phys.* **1994**, *188*, 247.
- (21) Onkelinx, A.; De Schryver, F. C.; Viaene, L.; Van de Auweraer, M.; Iwai, K.; Yamamoto, M.; Ichikawa, M.; Masuhara, H.; Maus, M.; Rettig, W. *J. Am. Chem. Soc.* **1996**, *118*, 2892.
- (22) Herbich, J.; Kapturkiewicz, A. *Chem. Phys.* **1993**, *170*, 221.
- (23) Soujanya, T.; Fessenden, R. W.; Samanta, A. *J. Phys. Chem.* **1996**, *100*, 3507.
- (24) Grabowski, Z. R.; Rotkiewicz, K.; Siemiarz, A.; Cowley, D. J.; Baumann, W. *Nouv. J. Chim.* **1979**, *3*, 443.
- (25) Valeur, B.; Bourson, J.; Pouget, J. In *Fluorescent Chemosensors for Ion and Molecule Recognition*; Czarnik, A. W., Ed.; ACS Symposium Series No. 538; American Chemical Society: Washington, DC, 1992.
- (26) Delmond, S.; Létard, J.-F.; Lapouyade, R.; Mathevet, R.; Jonusauskas, G.; Rullière, C. *New J. Chem.* **1996**, *20*, 861.
- (27) Wiessner, A.; Hüttmann, G.; Kühnle, W.; Staerk, H. *J. Phys. Chem.* **1995**, *99*, 14923.
- (28) Dobkowski, J.; Waluk, J.; Yang, W.; Rullière, C.; Rettig, W. *New J. Chem.* **1997**, *21*, 429.
- (29) Baumgarten, M.; Gherghel, L.; Friedrich, J.; Jurczok, M.; Rettig, W. *J. Phys. Chem. A* **2000**, *104*, 1130.
- (30) Verbouwe, W.; Van der Auweraer, M.; De Schryver, F. C.; Piet, J. J.; Warman, J.-M. *J. Am. Chem. Soc.* **1998**, *120*, 1319.
- (31) (a) Suenaga, H.; Nakashima, K.; Mizuno, T.; Takeuchi, M.; Hamacchi, I.; Shinkai, S. *J. Chem. Soc., Perkin Trans. 1* **1998**, 1263. (b) Regnouf de Vains, J.-B.; Papet, A. L.; Marsura, A. *J. Heterocycl. Chem.* **1994**, *31*, 1069.
- (32) Fages, F.; Desvergne, J.-P.; Bouas-Laurent, H. *J. Am. Chem. Soc.* **1989**, *111*, 96.
- (33) Melhuish, W. H. *J. Phys. Chem.* **1961**, *65*, 229.
- (34) Parker, C. A. *Photoluminescence of Solutions*; Elsevier: Amsterdam, 1968.
- (35) AMPAC 6.0; Semichem, 7204, Mullen, Shawnee, KS 66216, 1997. Dewar, M. J. S.; Zebisch, E. G.; Healy, E. F.; Stewart, J. P. *J. Am. Chem. Soc.* **1985**, *107*, 3902.
- (36) Berlman, I. B. *Handbook of Fluorescence Spectra of Aromatic Molecules*; Academic Press: New York, 1971; p 383.
- (37) (a) Rehm, D.; Weller, A. *Isr. J. Chem.* **1970**, *8*, 259. (b) Weller, A. *Z. Phys. Chem. N. F.* **1982**, *133*, 92.
- (38) The polarographic half-wave potentials of one-electron oxidation of pyrene and reduction of bpy were taken as +1.28 and -2.10 V/SCE in acetonitrile, respectively.<sup>38,39</sup>
- (39) Netzel, T. L.; Zhao, M.; Nafisi, K.; Headrich, J.; Sigman, M. S.; Eaton, B. E. *J. Am. Chem. Soc.* **1995**, *117*, 9119.
- (40) Elliott, C. M.; Hershenhart, E. J. *J. Am. Chem. Soc.* **1982**, *104*, 7519.
- (41) Birks, J. B. *Photophysics of Aromatic Molecules*; Wiley-Interscience: New York, 1970.
- (42) Nijegorodov, N. I.; Downey, W. S. *J. Phys. Chem.* **1994**, *98*, 5639.
- (43) Strickler, S. J.; Berg, R. A. *J. Chem. Phys.* **1962**, *37*, 814.
- (44) Van der Auweraer, M.; Grabowski, Z. R.; Rettig, W. *J. Phys. Chem.* **1991**, *95*, 2083.
- (45) (a) Maus, M.; Rettig, W.; Jonusauskas, G.; Lapouyade, R.; Rullière, C. *J. Phys. Chem. A* **1998**, *102*, 7393. (b) Maus, M.; Rettig, W. *Chem. Phys.* **1997**, *218*, 151.
- (46) In the case of 4'-(1-pyrenyl)acetophenone,<sup>28</sup> the calculations of the excited surface showed little dependence on the twist angle between phenyl ring and COCH<sub>3</sub> group.
- (47) Scaiano, J.-C. In *CRC Handbook of Organic Photochemistry*; Scaiano, J. C., Ed.; CRC Press: Boca Raton, FL, 1989; Vol. 1, p 343.